# Characterization and Photopolymerization of Divinyl Fumarate

**Huanyu Wei,[†] Tai Yeon Lee,[†] Wujian Miao,[‡] Ryan Fortenberry,[§] David H. Magers,[§] Sukhendu Hait,[†] Allan C. Guymon,[⊥] Sonny E. Jönsson,[#] and Charles E. Hoyle*[,†]**

*School of Polymer Science and High Performance Materials, University of Southern Mississippi, Hattiesburg, Mississippi 39406; Department of Chemistry and Biochemistry, University of Southern Mississippi, Hattiesburg, Mississippi 39406; Department of Chemistry and Biochemistry, Mississippi College, Box 4036, Clinton, Mississippi 39058; Department of Chemical and Biochemical Engineering, University of Iowa, Iowa City, Iowa 52242-1527; and Fusion UV Systems, Gaithersburg, Maryland 20878*

*Received February 8, 2007; Revised Manuscript Received May 22, 2007*

ABSTRACT: A complete characterization of the electron density distribution of divinyl fumarate and its effect on various properties has been performed by using a combination of UV−vis spectroscopy, cyclic voltammetry, theoretical calculations, and a diagnostic Michael addition reaction involving an aliphatic thiol and the fumarate carbon−carbon double bond. The results show that the presence of the conjugation between the two vinyl ester double bonds and the fumarate carbon−carbon double bond significantly changes the electron density in both; that is, the vinyl ester double bonds of divinyl fumarate are more electron rich and the fumarate double bonds are more electron poor compared to nonconjugated analogues. This electron density distribution greatly influences the copolymerization behavior of divinyl fumarate. Divinyl fumarate also acts as both a monomer and photoinitiator in the photopolymerization of 1,6-hexanediol diacrylate. Because of the larger electron density deficiency of the fumarate group on divinyl fumarate compared to its saturated analogue, diethyl fumarate, there is a reduced propensity of the fumarate group to copolymerize with electron-deficient acrylate groups. Finally, the fundamental photocleavage reaction of vinyl fumarate that leads to initiating radicals was determined by chemical trapping (2,2,6,6-tetramethyl-1-piperidinyloxy free radical, TEMPO) to be the primary α-cleavage process between the carbonyl carbon and the vinyl ester oxygen.

## Introduction

As photoinitiated polymerization began to expand in the 1970s, it became apparent that rapid polymerizing monomers that could be readily converted into network structures via a free-radical chain process upon exposure to UV light were essential.[1−4] While styrene, methacrylates, vinyl esters, dialkyl fumarates/maleates, and even *N*-vinyl amides polymerize via a free-radical chain process, their conversion rates are slow. Acrylates, on the other hand, polymerize rapidly via a free-radical chain process.[5] During the past two decades, there has been considerable activity[6−9] designed to alter the structures of acrylates and methacrylates to achieve even greater polymerization rates by synthesis of monomers with groups that are remote from the acrylate double bond; i.e., functional groups with various heteroatoms have been attached primarily to the terminal carbon of the alkyl side group (typically at the $\beta$-carbon of an ethyl group) of the acrylate ester. Recently, the photopolymerization of vinyl acrylate has shown it to be a very unique monomer with significantly altered copolymerization kinetics compared to traditional acrylate and vinyl ester monomers, and it is photochemically labile and serves as a photoinitiator.[10−12] Significant differences in the addition rates of external free radicals to the acrylate and vinyl ester double bonds of vinyl acrylate, compared to traditional acrylate and vinyl ester monomers, have been observed.[13] These differences result from the presence of both acrylate and vinyl groups on the same molecule, presumably due to some type of $\pi$-conjugation. In addition to altering the chemical reactivity of the vinyl ester and acrylate double bonds, the resultant conjugation also results in a red shift in the UV absorption that apparently generates free radicals by a photoscission process (Norrish I type) in the absence of added photoinitiators; hence, its utility as an effective photoinitiating monomer. Unfortunately, vinyl acrylate has an extremely low boiling point, thereby reducing its usefulness in photocurable systems.

It would be expected that analogues of vinyl acrylate with higher molecular weight and greater double bond conjugation would also exhibit similar UV absorption and enhanced reactivity behavior. Recently, monovinyl fumarate, divinyl fumarate, and divinyl maleate have been synthesized, and their use as self-initiating photoinitiators and commoners has been described in a short communication.[14] These novel vinyl esters exhibit red-shifted UV absorption compared to vinyl acrylate. In particular, divinyl fumarate (DiVF; structure given in Chart 1) is characterized by strong UV absorption at wavelengths greater than 300 nm, a critical property for efficient photoinitiators. In addition, DiVF at low concentrations has been shown to efficiently initiate acrylate photopolymerization; however, at the low concentrations reported,[14] the DiVF monomer is rapidly consumed by copolymerization with the acrylate leading to its loss after relatively modest acrylate conversions are attained.

In view of the above considerations of monomers with enhanced reactivity and the ability to initiate free-radical via a photolysis process, we present detailed results for the characterization of DiVF as both a monomer and photoinitiator. Characterization includes chemical structural analysis via cyclic

* To whom correspondence is to be addressed: e-mail Charles.Hoyle@usm.edu; Ph 601-266-4873; Fax 601-266-5504.
† School of Polymer Science and High Performance Materials, University of Southern Mississippi.
‡ Department of Chemistry and Biochemistry, University of Southern Mississippi.
§ Mississippi College.
⊥ University of Iowa.
# Fusion UV Systems.

10.1021/ma070344a CCC: $37.00 
Published on Web 07/24/2007

**Chart 1. Chemical Structures of (a) DiVF, (b) DiEF, (c) VDEC, (d) VPRO, (e) HDDA, (f) DMPA, (g) TEGDVE, and (h) E3M**

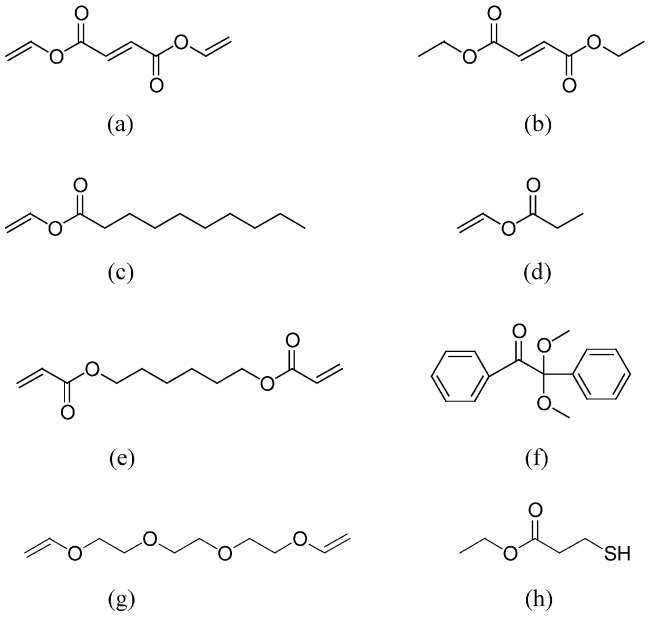


voltammetry and theoretical calculations as well as an assessment of DiVF chemical reactivity in both small molecule reactions and free-radical polymerization processes. The results presented herein provide a clear rationale for the photochemical reactivity of DiVF and the inherent propensity of the electronically coupled double bonds to participate in free-radical chain reactions.

## Experimental Section

**Materials.** 1,6-Hexanediol diacrylate (HDDA), dimethyl sulfoxide (DMSO), and 2,2-dimethoxy-2-phenylacetophenone (DMPA) were obtained from Cytec, Fisher Chemicals, and Ciba Specialty Chemical, respectively. Ethyl 3-mercaptopropionate (E3M), diethyl fumarate (DiEF), vinyl decanoate (VDEC), vinyl propionate (VPRO) and triethylene glycol divinyl ether (TEGDVE) were obtained from Aldrich Chemicals. All chemicals were used as received without further purification. Divinyl fumarate (DiVF) was synthesized by transesterification between vinyl acetate and fumaric acid in the presence of a palladium catalyst.[14] The chemical structures of DiVF, DiEF, VDEC, VPRO, HDDA, DMPA, TEGDVE, and E3M are shown in Chart 1.

**Characterization.** UV absorption spectra in hexane solution were measured using a Cary 5 spectrometer. Cyclic voltammetric (CV) experiments were performed with a model 990B electrochemical scanning microscope (CH Instruments, Austin, TX). A conventional three-electrode cell was used, with a Pt wire as the counter electrode, $Ag/Ag^+$ (10 mM $AgNO_3$−0.10 M tetra-*n*-butylammonium perchlorate (TBAP) in $CH_3CN$) as the reference electrode, and a 2 mm in diameter Pt disk electrode or 3 mm glassy carbon (GC) electrode as the working electrode. Acetonitrile ($CH_3CN$, >99.93%, HPCL grade, Sigma-Aldrich) or dimethyl sulfoxide (DMSO, >99.9%, Sigma) with TBAP (electrochemical grade, Fluka, 0.10 M in DMSO) was used as the electrochemical solvent and electrolyte, respectively. All solutions were degassed with high-purity $N_2$ for ∼15 min, and the working electrode was polished with 0.3 $\mu$m alumina slurry and then washed and dried before each CV. All experiments were conducted at a room temperature of 20 ± 2 °C.

**Molecular Orbital Calculations.** Ab initio molecular orbital theory calculations were performed at the level of second-order perturbation theory (MP2)[15] employing the 6-311+G(d,p) basis set.[16−18] This basis set comprises the standard triple-$\zeta$ valence 6-311G split-valence set, d polarization functions on all non-hydrogen atoms and p polarization functions on hydrogen, and additional, diffuse s and p functions on all non-hydrogen atoms. In particular, Mulliken population analyses[19] were performed, and molecular orbital energies of frontier orbitals were examined. All calculations were performed using the Gaussian03 program package.[20]

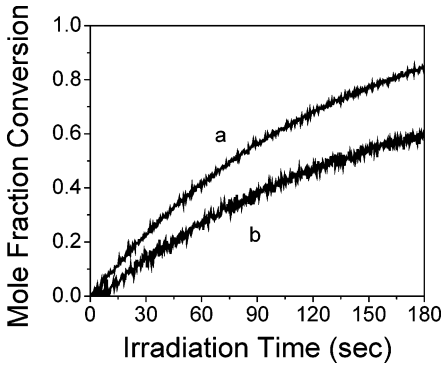


**Figure 1.** Mole conversions vs time plot of DiEtF/VDEC (a) fumarate and (b) vinyl ester 1:2 molar mixtures at 60 °C. Irradiance is 14 mW/cm$^2$ at 365 nm. DMPA (1 wt %) was used as a photoinitiator.

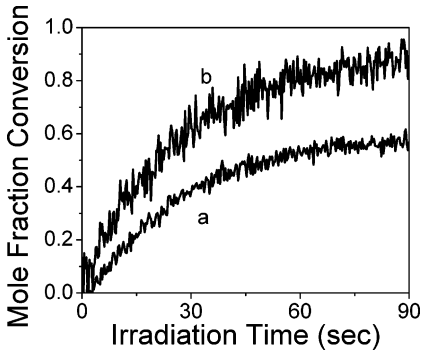


**Figure 2.** Mole conversions vs time plot of DiVF (a) fumarate and (b) vinyl ester at 60 °C. Irradiance is 14 mW/cm$^2$ at 365 nm. DMPA (1 wt %) was used as a photoinitiator.

**Photopolymerization.** The photopolymerization kinetic profiles during the UV-induced free-radical polymerizations were recorded using real-time infrared (RTIR) spectroscopy on a modified Bruker 88 FTIR spectrometer designed to allow light to impinge on a horizontal sample using a fiber-optic cable as a function of irradiation time. A 200 W high-pressure mercury−xenon lamp (Oriel) served as the light source. Conversion rates of each bond were calculated according to disappearance of IR absorption bands: 812 cm$^{-1}$ for the acrylate of HDDA, 2570 cm$^{-1}$ for the thiol of E3M, 764 cm$^{-1}$ for fumarate of DiVF, 980 cm$^{-1}$ for fumarate of DiEF, 885 cm$^{-1}$ for the vinyl ester of DiVF, and 870 cm$^{-1}$ for the vinyl esters VDEC and VPRO.

**Amine-Catalyzed Michael Addition Reaction.** A 1:1 molar ratio of DiVF or diethyl fumarate and E3M was mixed at room temperature in nitrogen conditions. Before adding 1 mol % of diethylamine, IR of the mixtures between two NaCl salt plates was obtained. After mixing with the amine, IR spectra were measured at 30 and 60 s. IR absorption of the thiol peak and the fumarate peak were measured and normalized with the height of $CH_2$ stretching peak as an internal standard to compensate for variation in sample thickness between samples. Then, conversions were calculated from normalized absorbance changes of thiol and fumarate peaks.

**Chemical Trapping of Initiating Radical.** DiVF (1 mmol) and 2,2,6,6-tetramethyl-1-piperidinyloxy free radical (TEMPO) (10 mmol) were dissolved in hexane in a quartz tube and degassed with nitrogen at −5 °C for 20 min to produce an oxygen-free system. The mixture was photolyzed using 365 nm UV light for 2 h in a Rayonet photochemical reactor (The Southern New England Ultraviolet Co.). The majority of unreacted TEMPO was removed

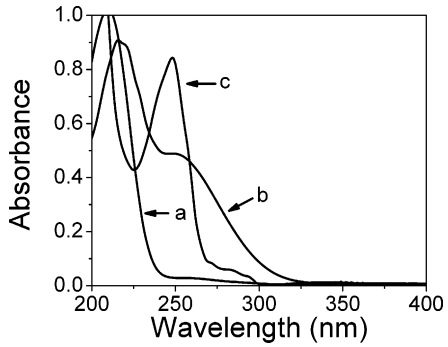


**Figure 3.** UV absorption spectra of (a) DiEF, (b) DiVF, and (c) DMPA in hexane solution with equal molar concentration.

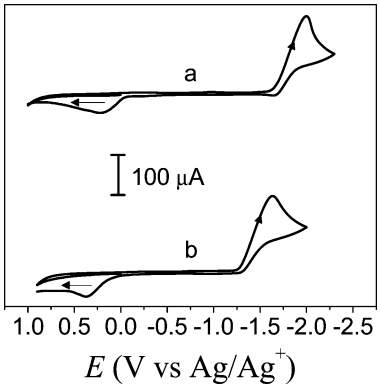


**Figure 4.** Cyclic voltammograms obtained from a 0.10 M TBAP DMSO solution containing (a) 61 mM DiEF and (b) 83 mM DiVF at 2 mm in diameter Pt electrode with a scan rate of 100 mV/s. For clarity, the current was multiplied by 1.5 for (b).

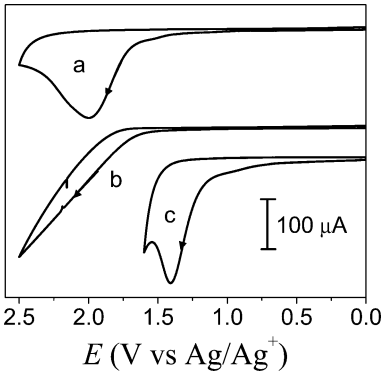


**Figure 5.** Cyclic voltammograms obtained from (a) 73 mM DiVF, (b) 85 mM VDEC and (c) 88 mM TEGDVD and in 0.10 M TBAP $CH_3CN$ solution at 3 mm in diameter GC electrode with a scan rate of 100 mV/s. For clarity, the current was multiplied by 2.5 for (a), 0.40 for (b), and 0.7 for (c).

by sublimation under reduced pressure. The chemical structure of the photolyzed product was analyzed by $^1H$ and $^{13}C$ NMR (200 MHz, Bruker) including correlated spectroscopy (COSY) and the distortionless enhancement by polarization transfer (DEPT) technique.

## Results and Discussion

The chemical structures of all components used in this investigation including DiVF and corresponding models are shown in Chart 1. After considering critical aspects of its inherent polymerization in free-radical polymerization using an external photoinitiator to initiate polymerization, characterization of DiVF with respect to the electron density of the fumarate internal double bond and the two vinyl ester terminal double bonds will be presented. Characterization techniques include

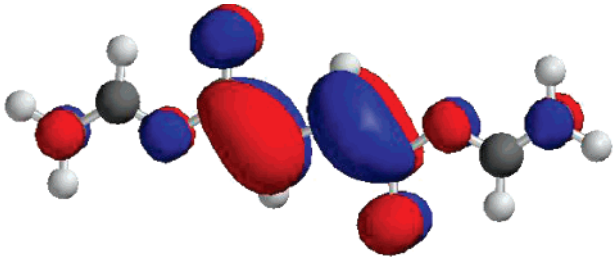

**Figure 6.** Plot of the lowest unoccupied molecular orbital (LUMO) for DiVF—the $\pi$ antibonding orbital of the fumarate double bond.

**Table 1. Molar Extinction Coefficients (L/(mol cm)) of DiEF, DiVF, and DMPA at 254, 313, and 366 nm**

| | 254 nm | 313 nm | 366 nm |
|---|---|---|---|
| DiEF | 407.94 | 77.66 | 9.28 |
| DiVF | 6872.62 | 485.31 | 123.94 |
| DMPA | 9329.7 | 81.1 | 107.47 |

UV−vis spectroscopy, a catalyzed diagnostic reaction with a monoalkylthiol, electrochemical measurement of the reduction (fumarate) and oxidation (vinyl ester) of DiVF in comparison to a traditional dialkyl fumarate and vinyl alkylate, a Mulliken electron population analyses from molecular orbital calculations of the terminal double bonds in DiVF compared to those in VDEC and TEGDV, and calculation of the LUMO energies for DiVF and its analogue DiEF. Next, the photopolymerization kinetics of a diacrylate monomer [1,6-hexanediol diacrylate (HDDA)] with increasing DiVF concentration is reported using real-time infrared (RTIR) spectroscopy to follow all polymerizable functionalities including acrylate, fumarate, and vinyl ester double bond conversions. The effect of the DiVF concentration on the conversion of HDDA is hence established. Finally, a radical photoproduct was identified by reaction with a radical trap.

**Photopolymerization of DiVF and DiEF/VDEC Mixtures.** In order to establish a sound basis for the characterization of DiVF as a monomer participating in free-radical polymerization processes, we first present results for the photopolymerization of DiVF and a model system comprised of a mixture of diethyl fumarate (DiEF) with vinyl decanoate (VDEC) by excitation of an added external photoinitiator. Results for the use of DiVF as a photoinitiator will be relegated to a later section. Figure 1 shows the mole fraction conversions of fumarate and vinyl groups vs exposure time to the 366 nm output (14 mW/cm$^2$) of a filtered medium-pressure mercury lamp for 1:1 and 1:2 molar mixtures of DiEF and VDEC with 1 wt % DMPA photoinitiator. In both cases the mole fraction conversion rate of fumarate double bonds is higher than the mole fraction rate of vinyl ester groups: note that the mole fraction conversion plot for VDEC in Figure 1b had to be adjusted (multiplied by a factor of 2) before comparison with the fumarate molar conversion could be made due to the higher molar concentration of VDEC. The results in Figure 1 are consistent with reactivity ratios of $r_1 = 0.44$ and $r_2 = 0.011$ for the copolymerization of DiEF (component 1) with typical vinyl alkonates reported in the literature.[21] Before proceeding to results for DiVF, we point out that the initial conversion rate for the fumarate double bond (0.0076 mol L$^{-1}$ s$^{-1}$) is greater than for the vinyl ester double

**Table 2. Mulliken Population Numbers of Carbons in Terminal Vinyl Ester Double Bonds of VDEC, DiVF, and TEGDVE**

| | Mulliken population of carbons |
|---|---|
| VDEC | −0.188 |
| DiVF | −0.215 |
| TEGDVE | −0.384 |

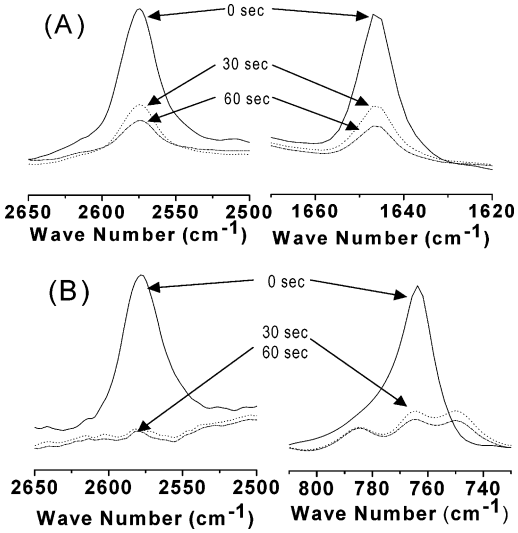


**Figure 7.** FTIR spectra changes of thiol and fumarate double bonds of (A) DiEF/E3M and (B) DiVF/E3M 1:1 molar mixtures during an amine-catalyzed Michael reaction.

**Table 3. Percent Conversion of Thiol and Fumarate from Amine-Catalyzed Michael Reactions of DiEF/E3M and DiVF/E3M Mixtures as a Function of Time**

| | E3M/DiEF | | E3M/DiVF | |
|---|---|---|---|---|
| time (s) | thiol (%) | fumarate (%) | thiol (%) | fumarate (%) |
| 0 | 0 | 0 | 0 | 0 |
| 30 | 63.3 | 61.6 | 97.7 | 94.8 |
| 60 | 73.8 | 75 | 98.3 | 95.7 |

bond (0.0054 mol $L^{-1}$ $s^{-1}$) for the 1:2 molar ratio of fumarate: vinyl ester. The results in Figure 1b are a model for the DiVF results to be presented next. In Figure 2, plots of the fumarate and vinyl ester group mole fraction conversion vs time for DiVF upon exposure to the same lamp source intensity and photoinitiator concentration used for the DiEF/VDEC mixture indicate that the molar conversion (if adjusted for the 1:2 molar fumarate: vinyl ester initial double bond ratio) of the vinyl ester is greater than the molar conversion of the fumarate. Furthermore, the initial rate of conversion of the vinyl ester group of DiVF (0.0239 mol $L^{-1}$ $s^{-1}$) is greater than for the fumarate group (0.0165 mol $L^{-1}$ $s^{-1}$). We quote the initial rates for DiVF since at this point in the reaction all of the fumarate and vinyl ester groups present are conjugated. As the polymerization proceeds, there will be a mixture of conjugated fumarate and vinyl ester double bonds on unreacted DiVF as well as nonconjugated fumarate and vinyl ester groups resulting from reaction of the "other double bond" on DiVF. Bearing this in mind, comparing the results in Figure 2 for DiVF to those in Figure 1b for 1:2 DiEF:VDEC and concentrating on the results at low conversion, it is apparent that the reactivities of the DiVF double bonds are markedly different than their DiEF and VDEC counterparts. We have suggested in a previous communication[14] that the DiVF fumarate double bond is much more electron poor than the fumarate double bond of DiEF, and concomitantly the DiVF vinyl ester double bonds are more electron rich than the vinyl ester double bonds of traditional vinyl alkanoates such as vinyl acetate, vinyl propionate, or vinyl decanoate. In the next sections we present a complete chemical and theoretical description of the electron density of the fumarate and vinyl ester bonds in DiVF.

**Characterization of DiVF: Absorbance and Extinction Coefficients.** As shown in Figure 3, DiVF exhibits strong UV absorption at wavelengths longer than 300 nm, extending to greater than 350 nm. The red shift in absorption compared to dialkyl fumarates is a result of an extended conjugation involving the vinyl ester and fumarate carbon−carbon double bonds and the intermediate carbonyl. Because UV light sources traditionally provide strong intensities at 254, 313, and 366 nm, molar extinction coefficients ($\epsilon$) at these wavelengths are an important aspect of a chromophores overall ability to initiate photopolymerization upon exposure to mercury light. For direct comparison, Table 1 shows the molar extinction coefficients ($\epsilon$) of DiVF, DiEF, and DMPA at 254, 313, and 366 nm in hexane. Compared with DiEF, DiVF has much higher $\epsilon$ values at all three wavelengths. The extinction coefficient at 254 nm of DiVF is about 26% lower than that of DMPA. However, $\epsilon$ for DiVF is ~6 times greater than the value of $\epsilon$ for DMPA at 313 nm. The n, $\pi^*$ absorption extinction coefficients at 366 nm are approximately the same for both DMPA and DiVF. This red-shifted absorbance for DiVF is a unique property for $\alpha,\beta$-unsaturated esters which is only found to exist when an unsaturated carbon−carbon double bond is on the oxygen ester: the same phenomenon is seen for vinyl acrylate,[11] ethyl vinyl fumarate, vinyl cinnamate, and vinyl crotonate as well as any similarly configured molecular architecture.

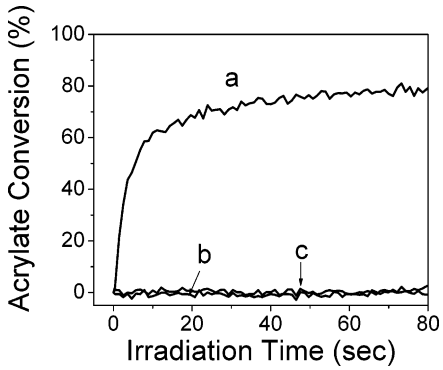


**Figure 8.** RTIR percent conversion vs time plots of HDDA polymerization in the presence of (a) 5 wt % of DiVF, (b) no photoinitiator, and (c) mixture of DiEF and VPRO equivalent to 5 wt % of DiVF. Light intensity (full arc) is 187 mW/$cm^2$.

**Characterization of DiVF: Cyclic Voltammetry.** Probably the best method of characterizing the electronic nature of the double bonds in a reactive chemical species is to measure its oxidation and reduction profiles. Accordingly, cyclic voltammograms of DiVF and its monomolecular saturated analogues DiEF and VDEC were recorded in $CH_3CN$ (oxidation at GC) or DMSO (reduction at Pt) at room temperature using a conventional three-electrode cell, with a Pt wire as the counter electrode, $Ag/Ag^+$ (10 mM $AgNO_3$−0.10 M TBAP in $CH_3CN$) as the reference electrode, and either a 2 mm diameter Pt or a 3 mm diameter GC electrode as the working electrode.

As can be seen in Figure 4, comparison of the reduction waves of DiVF and DiEF indicates that it is much easier to reduce the fumarate group of DiVF than DiEF. The reduction peak potentials are located at −2.00 V vs $Ag/Ag^+$ (Figure 4a) for DiEF and −1.63 V vs $Ag/Ag^+$ (Figure 4b) for DiVF at a Pt electrode in DMSO with a scan rate of 100 mV/s. This large difference in reduction peak potentials clearly indicates that the fumarate double bond of DiVF, as expected, is much more electron deficient than DiEF. On the reverse scans, a small reoxidation wave around −1.7 V vs $Ag/Ag^+$ is observed for DiEF, but not DiVF. When relatively high scan rates (200−500 mV/s) were employed, the peak ratio of the reoxidation to reduction was slightly increased for DiEF; however, for DiVF the reoxidation wave did not appear with the faster scan rate. The reduction processes are probably attributed to one-electron

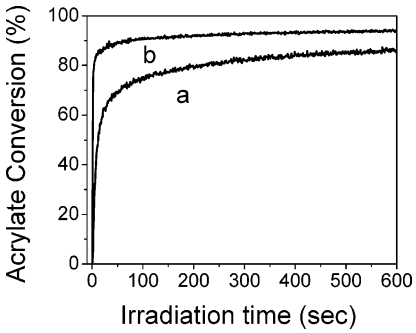


**Figure 9.** RTIR percent conversion vs time plots of HDDA polymerization in the presence of 1 mol % of (a) DiVF and (b) DMPA. Light intensity (full arc) is 187 mW/cm$^2$.

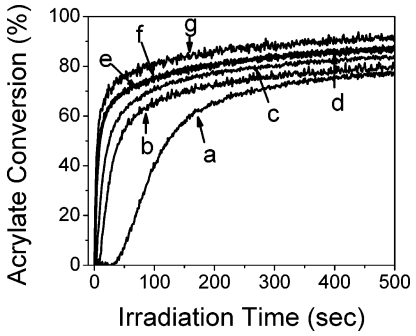


**Figure 10.** RTIR percent conversion vs time plots of HDDA polymerization in the presence of (a) 0.01, (b) 0.05, (c) 0.1, (d) 0.5, (e) 1, (f) 2, and (g) 5 wt % of DiVF. Light intensity (full arc) is 187 mW/cm$^2$.

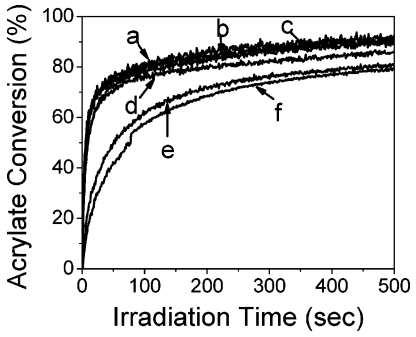


**Figure 11.** RTIR percent conversion vs time plots of HDDA polymerization in the presence of (a) 5, (b) 10, (C) 20, (d) 30, (e) 40, and (f) 50 wt % DiVF. Light intensity (full arc) is 187 mW/cm$^2$.

electrochemical reductions followed by hydrodimerization chemical reactions.[22] The electrohydrodimerization products can be further oxidized at peak potential values of +0.21 and +0.37 V vs Ag/Ag$^+$ for DiEF and DiVF, respectively.

The oxidation of DiVF, and for comparison VDEC, was also evaluated in order to establish the electron density of the vinyl ester groups on DiVF with respect to the vinyl ester double bond on a representative saturated aliphatic vinyl ester. Figure 5 (curves a and b) shows the oxidation waves for DiVF and VDEC at the GC electrode in $CH_3CN$ with a scan rate of 100 mV/s. The oxidation wave for DiVF (Figure 5a) has a peak potential value of +2.0 V vs Ag/Ag$^+$, while the oxidation of VDEC (Figure 5b) never attains a peak within the potential window studied, suggesting that its oxidation peak potential is greater than 2.5 V! Hence, we conclude that the vinyl ester groups of DiVF are much more electron rich than the vinyl ester group of the standard aliphatic vinyl ester VDEC. For comparison, the oxidation wave for TEGDVE is shown in Figure 5c. The low positive oxidation peak potential of ~1.41 V vs Ag/Ag$^+$ for the vinyl ether indicates that while the vinyl ester double bond of DiVF is electron rich compared to the vinyl ester group of VDEC, it is still certainly not as electron rich as a conventional aliphatic vinyl ether double bond.

**Characterization of DiVF: Theoretical Calculations.** In order to provide additional evidence for the electron density of the vinyl ester double bonds of DiVF, theoretical calculations for DiVF, VDEC, and TEGDVE were made. A Mulliken population analysis is simply an algorithm for summing the electron density by atoms. Thus, a negative population indicates an electron density around that atom greater than the positive charge of that atom's nucleus. Results are presented in Table 2. Note that the calculations support the conclusions drawn from the oxidation potentials presented above. The vinyl ester double bond of DiVF is electron rich as compared to that of VDEC, but less than the double bonds of TEGDVE.

The population numbers of the carbons in the fumarate double bonds were too small for valid comparisons. Therefore, another result from the calculations was compared. For both of the two fumarates, DiVF and DiEF, the lowest unoccupied molecular orbital (LUMO) is the $\pi$ antibonding orbital of the fumarate double bond. Thus, reduction of each of these fumarates will occur most easily at the fumarate double bond. A plot of the LUMO for DiVF is shown in Figure 6. The energies for the LUMO in DiVF and DiEF are 15.41 and 27.86 kcal/mol, respectively. While these energies are certainly not quantitative, the trend is irrefutable and indicates that DiVF should be reduced much easier than DiEF. This is consistent with and provides a rationale for the reduction potentials obtained from cyclic voltammetry.

**Characterization of DiVF: Thiol Michael Addition to Fumarate Bond.** The lower electron density of the fumarate ene in DiVF (compared to the fumarate double bond in DiEF) as determined by cyclic voltammetry and substantiated by theoretical calculations can be evaluated directly by a diagnostic reaction used to probe double bond electron density. For thiol−ene Michael addition reactions, rates are inversely proportional to the ene electron density.[23,24] Therefore, the relative electron density of the fumarate double bond in DiVF compared to that of conventional fumarate esters can be determined by comparing thiol addition rates in the presence of a catalytic amine concentration. Indeed, the lower electron density of the acrylate group in vinyl acrylate compared to traditional acrylates has been previously determined by the lower reactivity of the acrylate group in an amine-catalyzed Michael addition of an aliphatic thiol with vinyl acrylate compared to reaction with traditional acrylates.[25] Figure 7 shows changes in the IR bands for thiol (2575 cm$^{-1}$) and the central ene fumarate groups (1646 cm$^{-1}$ for DiEF and 764 cm$^{-1}$ for DiVF) for the primary amine-catalyzed reaction between ethyl-3-mercaptopropionate (E3M; see Chart 1) and both DiVF and DiEF as a function of time after mixing. From the corresponding conversions of the fumarate and thiol groups listed in Table 3, it can be concluded that the catalyzed thiol addition to the central fumarate double bond of DiVF is much faster than to DiEF. For the DiVF/E3M mixture, little of the thiol or fumarate double bond is observed after only 30 s of reaction while the DiEtF/E3M mixture has approximately 36.7% thiol and 38.4% fumarate groups remaining after the same time period. It should be emphasized that essentially identical conversions for the fumarate and thiol groups indicate a stoichiometric 1:1 addition process, which is consistent with the results for primary amine-catalyzed Michael additions to acrylate double bonds.[25] These results herein clearly confirm the results found by cyclic voltammetry and theoretical

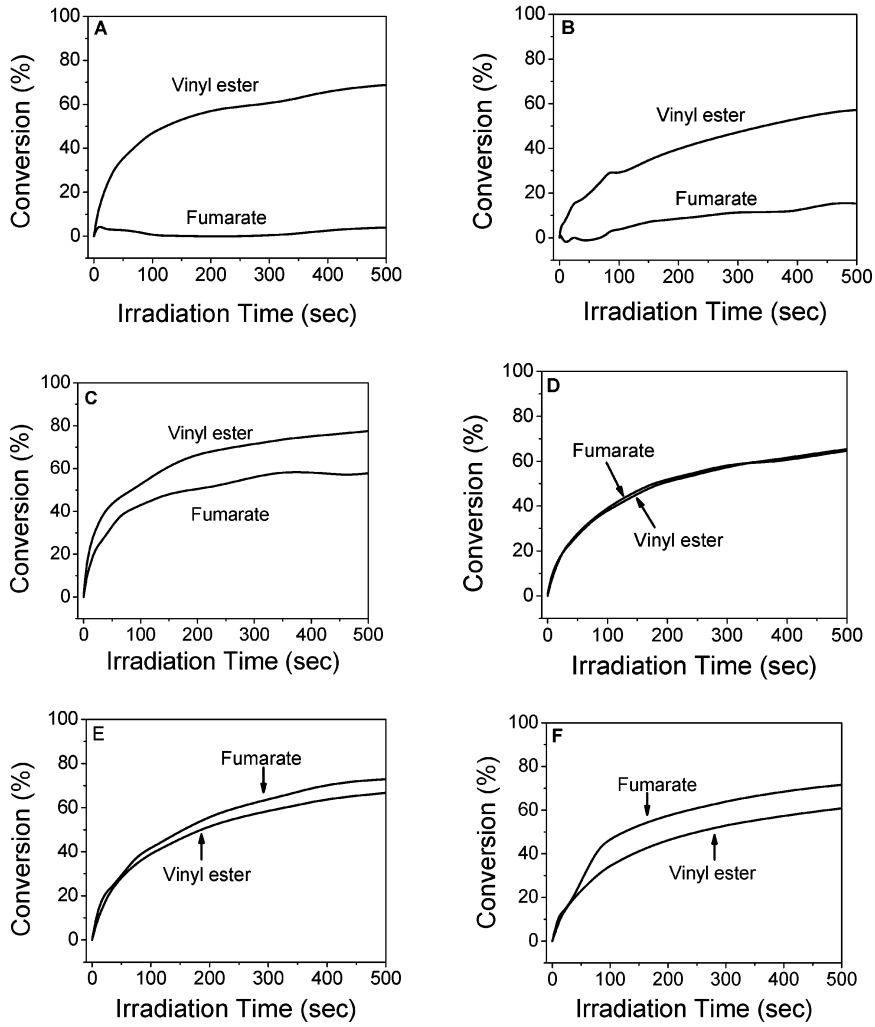


**Figure 12.** RTIR fumarate and vinyl ester percent conversion vs time plots of HDDA polymerization in the presence of (A) 5, (B) 10, (C) 20, (D) 30, (E) 40, and (F) 50 wt % DiVF. Light intensity (full arc) is 187 mW/cm$^2$.

calculations for the DiVF vs the DiEF fumarate double bond, i.e., the lower electron density of the fumarate group in DiVF manifests itself in faster reaction rates with the amine catalyzed thiol addition.

**Photopolymerization Kinetics and Initiation Process of HDDA/DiVF Mixtures: Conversion Rates.** To evaluate the effectiveness of DiVF simultaneously as an initiator and comonomer for the polymerization of HDDA, a comprehensive RTIR analysis of the polymerization process was conducted. First, HDDA was polymerized in the presence of low concentrations of DiVF to evaluate its inherent ability to initiate photopolymerization of HDDA. For comparison, DiEF and VPRO were added in equal concentrations as the DiVF to determine whether an intermolecular charge-transfer complex between vinyl ester and fumarate groups can form and initiate polymerization upon excitation with light. As shown in Figure 8, where all polymerizations were performed between two salt plates with only residual oxygen present, HDDA does not polymerize efficiently in the absence of a photoinitiator or in the presence of a 1:2 molar mixture of DiEF and VPRO (5 wt % DiVF equivalent), while the sample with 5 wt % DiVF polymerizes rapidly. This demonstrates that the presence of both fumarate unsaturation and vinyl ester groups on the same molecule is essential for initiating polymerization photolytically. The HDDA sample polymerizes quickly, attaining 70% conversion within 50 s, demonstrating the effectiveness of DiVF as a photoinitiator. To give an initial assessment of the efficiency of DiVF as a photoinitiator, it was compared with the standard cleavage photoinitiator DMPA. The conventional initiator DMPA has a higher initiating efficiency than DiVF at equal molar concentrations, as shown in Figure 9. It should be noted that the initiation ability of DiVF is actually better than it appears in Figures 8 and 9 since the concentration of DiVF decreases steadily by taking part in a copolymerization process, as will be discussed more fully later. It is important to note that the vast majority of DMPA remains unreacted after polymerization is complete, while DiVF, as we will show, readily polymerizes with the HDDA. Although the overall quantum yield for initiation of acrylate polymerization by DiVF is inherently lower (by a factor of between 20 and 30 according to initial rates for solutions with equal absorbance at 313 nm) than for the conventional photoinitiator DMPA, its ability to be incorporated into the polymer network by virtue of its participation in the free-radical polymerization process that it initiates could be an asset.

To expand the investigation of DiVF as a photoinitiator for acrylate polymerization, HDDA samples with concentrations of DiVF from 0.01 up to 50 wt % were next monitored using RTIR, as shown in Figures 10 and 11. The results in Figure 10 show that HDDA polymerizes to a conversion of ~70% in 500 s in the presence of only 0.01 wt % DiVF. The polymerization rate and conversion of HDDA continuously increase with an increase of DiVF concentration, attaining a maximum polymerization rate and conversion for a DiVF concentration of 5

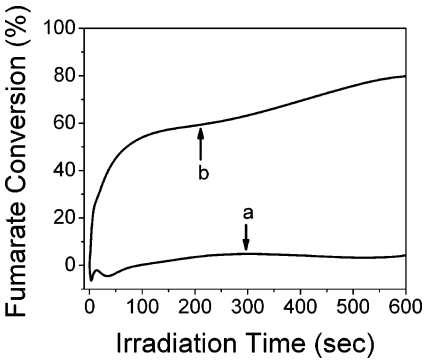


**Figure 13.** RTIR vinyl ester percent conversion vs time plots of 5% DiEF in (a) DMSO and (b) HDDA in the presence of 1 wt % DMPA. Light intensity (full arc) is 187 mW/cm$^2$.

wt %. Concentrations of DiVF greater than 5 wt % (Figure 11) exhibited a continual decrease in polymerization rate and conversion with an increase in DiVF concentration.

As we have already alluded, DiVF cannot only function as a photoinitiator, but it can also potentially be consumed by free-radical chain reactions involving both the fumarate and the vinyl ester double bonds. Thus, to complement the results in Figures 10 and 11, the conversion vs time plots rates for the fumarate and vinyl ester double bond with increasing concentrations of DiVF in HDDA were also monitored using RTIR, as shown in Figure 12. Focusing first on Figure 12A,B, it is readily noted that little or none of the fumarate is consumed, while the vinyl ester group readily copolymerizes with the acrylate as well as homopolymerizes to attain conversions of 50−70%. We note that there is some error associated with monitoring of the three bands (acrylate, fumarate, vinyl ester) in real time; nevertheless, while this introduces some uncertainty in the exact values for conversion of the vinyl ester functionalities in Figure 12 and the acrylate groups in Figures 10 and 11, we are confident of our ability to confirm the lack of any significant fumarate conversion for the 5 and 10 wt % DiVF/HDDA samples in Figure 12A,B. Once the DiVF reaches a concentration of 20 wt % or greater (Figure 12C−F), the fumarate double bond conversion becomes substantial due to the apparent copolymerization of the fumarate and vinyl groups on DiVF. It is also apparent from Figure 12 that at the lower DiVF concentrations (Figure 12A,B), the electron-deficient fumarate double bond in DiVF (as characterized in a previous section) does not readily copolymerize with the acrylate while the vinyl ester groups do. Since the concentration of the vinyl ester groups is also low in the 5 and 10 wt % samples, the inherent copolymerization rate between the fumarate and vinyl ester groups is not large enough to compete with the combination of the vinyl ester−acrylate copolymerization and the vinyl ester homopolymerization. To illustrate the effect of the low electron density of the fumarate group in DiVF, Figure 13a,b shows conversion vs time plots for 5 wt % DiEF in the unreactive solvent DMSO as well as in HDDA with 1 wt % DMPA photoinitiator in both. At a concentration of 5 wt %, DiEF does not homopolymerize in DMSO. However, in HDDA it readily copolymerizes with acrylate functional groups, in stark contrast to the electron-deficient fumarate groups in DiVF (see Figure 12A). Apparently, the electron-poor DiVF fumarate double bond will not copolymerize with acrylate groups which themselves are electron-poor. Another comparison for the DiVF results in Figure 12 is shown in Figure 14 for HDDA with DiEF and VPRO in a 1:2 molar ratio with the DiEF concentration set at concentrations of 5, 20, and 50 wt %. It is obvious from the results in Figure 14 for conversions of fumarate and vinyl ester groups as a function of time that, unlike the DiVF fumarate group, and like the results in Figure 13b, the fumarate conversion is rapid and attains a substantial conversion.

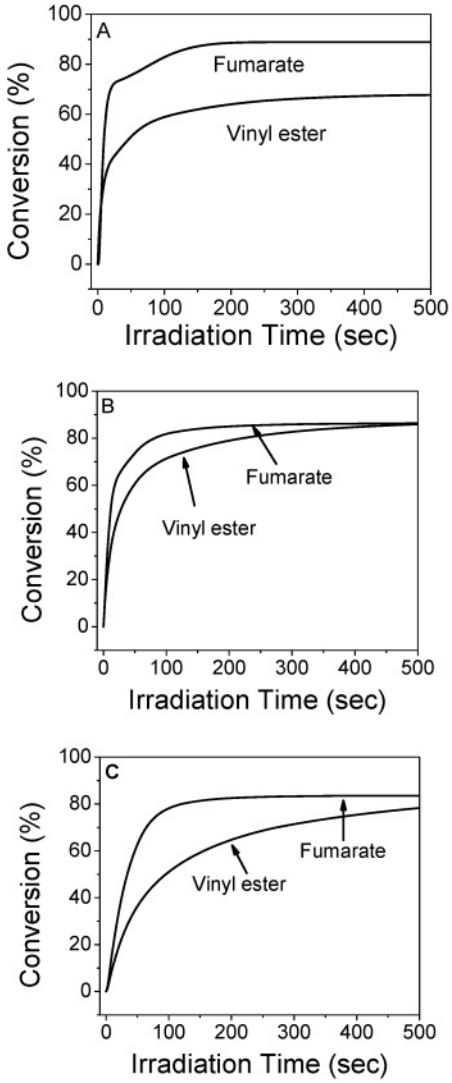


**Figure 14.** RTIR fumarate and vinyl ester percent conversion vs time plots of HDDA polymerization in the presence of DiEF and VP mixture (1:2 molar ratio) equivalent to (A) 10, (B) 20, and (C) 50 wt % DiVF. Light intensity (full arc) is 187 mW/cm$^2$.

**Initiation Mechanism.** As discussed previously, the UV absorption, self-initiation, and polymerization ability of self-initiating monomers are strongly dependent on monomer structure. In addition to the relationship between monomer structure and their polymerization kinetic profiles, elucidating the initiation mechanism is critical in leading to the development of better self-initiating monomers. We have chosen to use the traditional radical trap, TEMPO, whose structure is given in Scheme 1 to trap radicals produced by the photolysis of DiVF in a nonreactive solvent. Since TEMPO does not absorb light at 365 nm, the initiation mechanism of DiVF was examined by chemical trapping of the species produced by exposure of the DiVF solution using the 365 nm filtered light of a medium-pressure mercury lamp in the presence of a large excess amount of TEMPO. It is well-known that $\beta,\gamma$-unsaturated ketones undergo photoinduced rearrangement upon irradiation via an $\alpha$-cleavage reaction.[26] Using various NMR techniques, we have demonstrated that DiVF also undergoes a photoinduced $\alpha$-cleavage reaction generating two radicals, **1** and **2**, as shown in Scheme 1. Specifically, the trapped product, **4**, in the noncon-

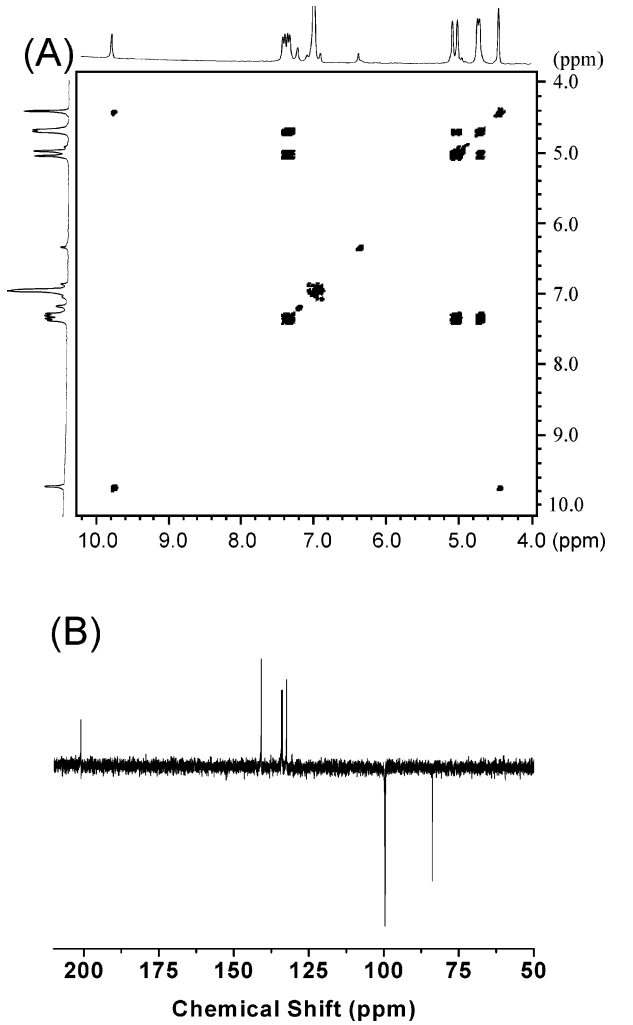


**Figure 15.** (A) $^1$H,$^1$H-COSY and (B) DEPT spectra of photolyzed product of DiVF in the presence of an excess amount of TEMPO.

**Scheme 1. Proposed Mechanism for Radical Formation upon DiVF Photolysis**

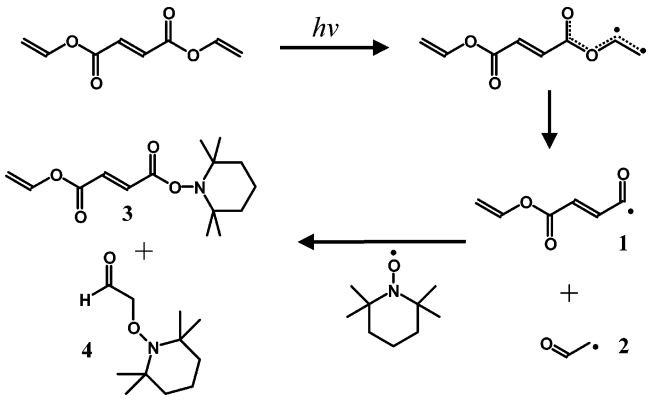


centrated photolyzed medium was determined by $^1$H, $^1$H-COSY (correlated spectroscopy), and DEPT (distortionless enhancement by polarization transfer) NMR techniques. Figure 15A shows the $^1$H,$^1$H-COSY spectrum of a photolyzed solution of DiVF. In addition to the peaks from unreacted DiVF [7.36 (quart, 1H, =CH vinyl), 7.0 (s, 1H, =CH fumarate), 5.04 (d, 2H, =CH*H* vinyl), and 4.73 (d, 2H, =C*H*H vinyl)], new peaks at 9.77 and 4.45 ppm were observed. The peaks at 9.77 and 4.45 ppm are from the aldehyde and methylene group in the trapped product, **4**. The correlation peak (9.77−4.45 ppm) of these two peaks indicates the presence of product **4**. The DEPT spectrum shown in Figure 15B [DEPT (200 MHz, $CDCl_3$) up (CH and $CH_3$) 200.1, 162, 140, 134, 100, down ($CH_2$) 83.8] also exhibits two new peaks, one upfield at 200.1 ppm (aldehyde, HCO−) and one downfield at 83.8 ppm (O=C$CH_2$O), clearly from product **4**. Both NMR analyses methods thus confirm the presence of product **4** in the photolyzed solution of DiVF. It was not possible to readily identify product **3** in the photolyzed mixture since it would have no distinctive shifts in either the $^1$H or $^{13}$C NMR spectrum compared to the original DiVF.

## Conclusions

Divinyl fumarate (DiVF) is a unique monomer that combines a fumarate double bond and two vinyl esters that are conjugated molecularly to provide a distinct red-shifted absorption spectrum that readily decomposes photolytically upon excitation. The radicals produced initiated free-radical polymerization not only of its own self, but also acrylate bonds. The basic polymerization reactivity of the vinyl ester and fumarate double bonds was altered compared to their unconjugated analogues. Specifically, the polymerization rate of the vinyl ester groups was faster than for the fumarate group. Just the opposite is true for the polymerization of diethyl fumarate and vinyl decanoate mixtures. Also, the fumarate double bond of DiVF does not polymerize at concentrations less than 10 wt % in a difunctional acrylate solution. The electron densities of the carbon−carbon double bonds in DiVF were characterized by cyclic voltammetry, molecular orbital calculations, and a diagnostic reaction with a primary amine-catalyzed addition of an aliphatic thiol to the fumarate. The electron density of the fumarate carbon−carbon double bond in DiVF is much lower than the fumarate double bond of diethyl fumarate. Likewise, the electron density of the vinyl ester double bond of DiVF is much greater than the electron density of the vinyl decanoate double bond. Upon photolysis DiVF undergoes an efficient α-cleavage process to give two radicals capable of initiating polymerization. The photoinitiation efficiency of DiVF is lower than that of a conventional cleavage photoinitiator, DMPA, on a per molar basis; however, unlike DMPA, the double bonds of DiVF are reactive and readily incorporated into the polymer network that they create. Finally, we reiterate that the results in this paper provide a general methodology for altering the reactivity of carbon−carbon double bonds by conjugation involving two double bonds and an ester linkage.

**Acknowledgment.** The authors acknowledge the support of Fusion UV Systems and NSF MRI-0321397 for part of this work.

## References and Notes

(1) Fouassier, J. P. *Photoinitiation Photopolymerization and Photocuring*; *Fundamentals and Applications*; Hanser Publishers: Munich, 1995.
(2) Fouassier, J. P.; Rabek, J. F. *Radiation Curing in Polymer Science and Technology*; Elsevier Applied Science: London, 1993.
(3) Roffery, C. G. *Photopolymerization of Surface Coatings*; Wiley-Interscience: New York, 1982.
(4) Pappas, S. P. *Radiation Curing, Science and Technology*; Plenum Press: New York, 1992.
(5) Anderson, H.; Gedde, U. W.; Hult, A. *Macromolecules* **1996**, *29*, 1649.
(6) Decker, C.; Muossa, K. *Eur. Polym. J.* **1991**, *27*, 881.
(7) Jansen, J. F. G. A.; Dias, A. A.; Dorshu, M.; Coussens, B. *Macromolecules* **2003**, *36*, 3861.
(8) Berchtold, K. A.; Nie, J.; Stansbury, J. W.; Hacioglu, B.; Beckel, E. R.; Bowman, C. N. *Macromolecules* **2004**, *37*, 3165.
(9) Beckel, E. R.; Stansbury, J. W.; Bowman, C. N. *Macromolecules* **2005**, *38*, 9474.
(10) Kudyakov, I. V.; Fos, W. S.; Purvis, M. B. *Ind. Eng. Chem. Res.* **2001**, *40*, 3092.

(11) Lee, T. Y.; Roper, T. M.; Jönsson, E. S.; Kudyakov, I.; Viswanathan, K.; Nason, C.; Guymon, C. A.; Hoyle, C. E. *Polymer* **2003**, *44*, 2859.
(12) Lee, T. Y.; Roper, T. M.; Jonsson, E. S.; Guymon, C. A.; Hoyle, C. E. *Macromolecules* **2004**, *37*, 3606.
(13) Mattias, W.; Khudyakov, I. V.; Turro, N. J. *J. Phys. Chem. A* **2002**, *106*, 1938.
(14) Lee, T. Y.; Guymon, C. A.; Jönsson, E. S.; Hait, S.; Hoyle, C. E. *Macromoloecules* **2005**, *38*, 7529−7531.
(15) Møller, C.; Plesset, M. S. *Phys. Rev.* **1934**, *46*, 618.
(16) McLean, A. D.; Chandler, G. S. *J. Chem. Phys.* **1980**, *72*, 5639.
(17) Krishnan, R.; Binkley, J. S.; Seeger, R.; Pople, J. A. *J. Chem. Phys.* **1980**, *72*, 650.
(18) Clark, T.; Chandrasekhar, J.; Spitznagel, G. W.; Schleyer, P. v. R. *J. Comput. Chem.* **1983**, *4*, 294.
(19) Mulliken, R. S. *J. Chem. Phys.* **1955**, *23*, 1833.
(20) Gaussian 03, Revision C.02: Frisch, M. J.; Trucks, G. W.; Schlegel, H. B.; Scuseria, G. E.; Robb, M. A.; Cheeseman, J. R.; Montgomery, J. A. Jr.; Vreven, T.; Kudin, K. N.; Burant, J. C.; Millam, J. M.; Iyengar, S. S.; Tomasi, J.; Barone, V.; Mennucci, B.; Cossi, M.; Scalmani, G.; Rega, N.; Petersson, G. A.; Nakatsuji, H.; Hada, M.; Ehara, M.; Toyota, K.; Fukuda, R.; Hasegawa, J.; Ishida, M.; Nakajima, T.; Honda, Y.; Kitao, O.; Nakai, H.; Klene, M.; Li, X.; Knox, J. E.; Hratchian, H. P.; Cross, J. B.; Adamo, C.; Jaramillo, J.; Gomperts, R.; Stratmann, R. E.; Yazyev, O.; Austin, A. J.; Cammi, R.; Pomelli, C.; Ochterski, J. W.; Ayala, P. Y.; Morokuma, K.; Voth, G. A.; Salvador, P.; Dannenberg, J. J.; Zakrzewski, V. G.; Dapprich, S.; Daniels, A. D.; Strain, M. C.; Farkas, O.; Malick, D. K.; Rabuck, A. D.; Raghavachari, K.; Foresman, J. B.; Ortiz, J. V.; Cui, Q.; Baboul, A. G.; Clifford, S.; Cioslowski, J.; Stefanov, B. B.; Liu, G.; Liashenko, A.; Piskorz, P.; Komaromi, I.; Martin, R. L.; Fox, D. J.; Keith, T.; Al-Laham, M. A.; Peng, C. Y.; Nanayakkara, A.; Challacombe, M.; Gill, P. M. W.; Johnson, B.; Chen, W.; Wong, M. W.; Gonzalez, C.; Pople, J. A. Gaussian, Inc., Wallingford, CT, 2004.
(21) Brandrup, J.; Immergut, E. H.; McDowell, W. *Polymer Handbook*, 2nd ed.; Wiley-Interscience: New York, 1975.
(22) (a) Michael, D. R.; Dennis, H. E. *J. Electrochem. Soc.* **1974**, *121*, 881. (b) Childs, W. V.; Maloy, J. T.; Keszthelyi, C. P.; Bard, A. J. *J. Electrochem. Soc.* **1971**, *118*, 874−880.
(23) Oswald, A. A.; Naegele, W. *Makromol. Chem.* **1996**, *97*, 258.
(24) Van Dijk, J. T. M. PCT Int Appl. 2000, 33.
(25) Lee, T. Y.; Kwang, W.; Jönsson, E. S.; Guymon, C. A.; Hoyle, C. E. *J. Polym. Sci., Part A: Polym. Chem.* **2004**, *42*, 4424.
(26) Turro, N. J. *Modern Molecular Chemistry*; University Science Books: Mill Valley, CA, 1991.

MA070344A